COMPUTER SIMULATION OF ANCHORING TECHNIQUE IN REINFORCED CONCRETE BEAMS

V.Cervenka and R.Pukl
Czech Technical University Prague

R.Eligehausen
Stuttgart University

SUMMARY

*The load transfer in reinforced concrete structures by means of anchoring elements is very common in modern concrete technology. Anchor*ing elements are often inserted in the bottom surface of a structure and the load is transfered by tensile action of the concrete. In case of shear failure, the anchores are located in the most exposed tensile zone of beams. The shear failure can be thus influenced by anchoring elements. This effect was analysed by means of the finite element program SBETA, which is based on the nonlinear-elastic constitutive model. The comparison with experiments for several loading configurations was made. In the second part a computer simulation of similar experiments was conducted.

1. INTRODUCTION

The wide spread use of anchoring elements in modern concrete technology requires the solution of a number of theoretical and practical questions, in order to ensure save and reliable applications. When using anchoring elements, the load is transfered into a reinforced concrete structure by means of metal anchors. The anchors and the surrounding concrete are subjected to significant tensile actions, which can influnce the behavior of the elements. In fact, the load carrying capacity of anchors in unreinforced concrete depends entirely on the concrete tensile strength. The traditional design methods are not applicable to this special problem, therefore new methods are being developed.

In recent years a large experimental program was conducted at the

Institute of Material Science in Building Construction of Stuttgart University under the guidance of the third author [1,2,3]. These experiments provided some important basis for design rules for anchor elements. It was found that loaded anchors located in the tensile zone of reinforced concrete beams decrease slightly the load carrying capacity of the beams. However, a rational explanation of the experimental behavior was not available.

The experiments indicated, that the failure is due to the concrete in the state of tension-compression. This type of failure cannot be succesfully analyzed by a simple beam theory. Therefore it was decided to exploit the recent advances in computational and fracture mechanics of concrete structures for the analysis of the problem.

The analysis was accomplished by a new finite element program SBETA, which was developed by the first two authors. The program is based on nonlinear-elastic material model with refined treatment of cracking. The program was used to analyze the experiments from the field of anchoring technique. The results indicated feasibility of the program for the analysis of the effect of anchoring elements. Subsequently, a parameter study was conducted, which simulated experiments of similar beams loaded through anchoring elements.

2. COMPUTER PROGRAM SBETA

The Computer program SBETA [4] is based on a finite element method with two-dimensional quadrilateral 4-node finite elements. Nonlinear solution technique enables a step-by-step loading of a structure. An iterative solution is performed at each load step until both, equilibrium and material laws are satisfied. It provides the informations about deformations, stresses, crack development and failure modes at each load step. The behavior of a structure can be traced in the serviceability as well as in failure states. The post-peak behavior of the structure is in many cases obtainable. The program is equiped with powerful graphical postprocessor. All important results, such as deformed state, stress and strain state, cracking and crushing of concrete, reinforcement yielding, can be presented graphically. Two solution methods, namely, the Newton-Raphson method and arch length method, are available. The later enables the analysis of the post-failure behavior, which is necessary for reliable determination of the maximum load and for the evaluation of the failure mode.

3. CONSTITUTIVE MODEL

The constitutive model of SBETA program is based on smeared approach. The material model for concrete has following characteristics:

- nonlinear behavior in compression with softening,
- bi-axial failure criterion,

- nonlinear fracture mechanics in tension,
- reduction of compressive strength after cracking,
- reduction of shear stiffness after cracking with variable shear retention factor,
- fixed and rotated crack models,
- tension stiffening effect due to bond.

Equivalent uniaxial law concept is used to calculate concrete elastic properties. The complete stress-strain law, Fig.1, is composed of second degree parabola in compression, linear tension and linear descending branches in tension and compression. The peak of the compressive curve, R_c, is derived from the bi-axial failure function by Kupfer at al. [5], Fig.2. The cracks start to form when tensile strength is reached. In tension-tension state the tensile strength is constant. In tension-compression state the tensile strength is reduced with increasing lateral compression. This relation is a hyperbola, which slightly deviates from the line between points $(s_1 = R_t, s_2 = 0)$ and $(s_1 = 0.2R_t, s_2 = R_c)$, where R_t, R_c are tensile and compressive strengths, respectively.

Before cracking the material is treated as isotropic, with modulus of elasticity derived from the equivalent uniaxial law using lowest principal stress. Poisson's ratio is assumed constant. After cracking, the material is orthotropic. The first material axis is normal to cracks and the second axis is parallel with cracks. The uniaxial law for each axis is considered independently. Two models for cracked concrete are possible: (a) rotated crack model, similar as suggested in [6], in which the principal axes of stresses and strains coincide, (b) fixed crack model, in which the material axes are fixed after crack initiation, Fig.3. In case of rotated crack model only two material components must be defined (concrete principal stresess), while in the fixed crack model three components must be defined on the crack plane.

The softening modulus in tension is adjusted to take into account the size effect. Bazant's formula [8] is used to calculate softening modulus E_t. This makes possible the transformation of the discrete crack behavior into the smeared constitutive model:

$$E_t = -\frac{R_t^2 h}{2G_f} \tag{1}$$

where h is the crack band width. This width is approximately related to element size by $h = \sqrt{A}$, where A is the element area. G_f is the fracture energy parameter. If G_f as is not known, an alterantive method si used to calculate softening modulus directly from tensile strength. Such relation was derived by Vos [9]. It takes advantage of the strong correlation

between fracture energy and tensile strength:

$$E_t = \frac{-R_t h}{w_0} \tag{2}$$

The constant w_0 represents the width of the discrete crack after complete loss of stress in case of linear softening. It is assumed invariant with respect to the concrete quality and equal to 0.051 mm.

Shear stiffness of the cracked concrete (in case of fixed crack model) is reduced using Kolmar's formula [10], which relates the shear retention factor β to the crack strain, Fig.4 :

$$G_c = \beta G_i, \qquad \beta = \frac{ln\,(e_1/c_1)}{c_2} \tag{3}$$

$$c_1 = 7 + 333\,(p - 0.005)\,, \qquad c_2 = 10 + 167\,(p - 0.005)$$

where G_i is the initial shear modulus of uncracked concrete, G_c is the Shear modulus of cracked concrete, and p is the reinforcing ratio of all reinforcement crossing the crack transformed into the crack plane. Furthermore, the shear stress on the crack plane can not exceed the tensile strength.

Compressive strength of the cracked concrete can be reduced as reported by Vecchio and Collins [7]. This effect is here modeled unsing linear relation as shown in Fig.5.

The contribution of the tensile stiffness of the concrete after cracking to the reinforcement stiffness, which is caused by bond properties of the reinforcement, is modeled by tension stiffening. The tension stiffening component t_s is a trilinear function, as shown in Fig.6. The first ascending part coincides with the range of the descending branche of the tensile stress-strain law for concrete. The middle constant part is a fraction of tensile strength of concrete (typically 0.4 R_t). The descending part starts, when the yielding of reinforcement begins. Tension stiffening component is calculated as an additional stress component. It is acting in direction of the reinforcement. Thus, in case of no reinforcement, no tension stiffening component is present. Unlike in some other models, tension stiffening is not included in the descending part of the concrete stress-strain law, and instead, it is considered separately.

4. EXPERIMENTAL BEAMS

The four experimental beams are illustrated in Fig.7. They are plate strips 0.6 m wide, 0.3 m thick, span 3.5 m and symmetrically loaded. Only longitudinal reinforcement and no vertical reinforcement is provided. Con-

crete cube strength was 20 MPa and high quality steel was used for reinforcing, in order to ensure concrete mode of failure. Bottom reinforcement was 6 bars diameter 15 mm, St 685/1080, top reinforcement was 4 bars diameter 12 mm, BSt 420/599 R. The beams 3.1.1 and 3.1.3 are loaded on the top surface as shown. In the beams H130/1 and H130/2 a half of the load is applied by means of the anchoring elements. In the beam H130/1 the anchors are located directly under the top loading forces, while in the beam H130/2 the anchors are located in the shear zone, between the top loading forces and the support. The beams are part of a large experimental program, Ref.[1],[2] The purpose of the tests was to investigate the effect of the loading applied by means of anchoring elements located in the tension zone of the beams on the load carrying capacity of the beams.

5. ANALYSIS OF EXPERIMENTAL BEAMS BY PROGRAM SBETA

Fig.8 shows the finite element model of the Beam 3.1.1. Only the left part of the symmetrical beam is analyzed. Three stages of analysis by a rotated crack model are illustrated. Fig.9 shows the comparison of the two analytical failure stages (rotated and fixed crack models) with the experiment. The deformed finite element mesh is shown. The cracks are schematically indicated by a line in the center of the elements. The thick lines indicate wide cracks. The filled-in elements indicate the concrete failure. This local failure was in all cases a compressive failure after tensile cracking, which is observed in experiments as explosive splitting. Apparently the rotated crack model represents more realistically the strain localization in the diagonal tension zone. However, both crack models give relatively good results. Fig.10 shows the same comparison for the Beam H1340/1 with anchoring elements.

Fig.11 shows the comparison of load-displacement diagrams for beams 3.1.1 and H130/1 as found by experiments (right diagram) and as calculated by finite element analysis. Good agreement between analytical and experimental results is found. The analysis can describe the reduction of the failure load of the beam with anchoring elements. This reduction was in experiment 0,92 and in FEM analysis 0,9. Similar conclusion can be drawn from the analysis of beams 3.1.3 and H130/2 shown in Fig.12 and 13. Here, the experimentally established reduction of the ultimate load due to loading through anchoring elements was 0,9 while the reduction found by FEM analysis was 0,86.

In spite of relatively good agreement, more detailed analysis disclosed some inconsistensies in the present formulation. The shear failure occures in the tension-compression stress state. The sequence of the failure (first cracking, then crushing, or first crushing) depends on small changes in the stress state. The present model, described in Sect.3 uses non-local

concept for tensile failure, but local formulation for compressive failure. Thus in case of compressive failure the mesh dependency should be expected. These problems are now being investigated by the authors with intention to improve the present formulation.

6. SIMULATION OF EXPERIMENTS

After verifying the numerical model by analyzing experimental beams, a parameter study was conducted with the aim of simulating laboratory experiments. A beam identical with the experiments described in Sect.4 was subjected to the three types of loading: top loading, anchor loading and the combination of both. The position of load on the beam was varied in order to study the effect of shear span ratio a/h. An example of failure stages for these three loading types is shown in Fig.14. The result of the computer simulation is illustrated by Fig.15, where the reduction of the ultimate moment at failure is plotted for variable shear span ratio and the three loading types. The ultimate moment reduction, known as the "Kani shear valley" is amplified if the anchor loading is present. The analysis of failure mode indicates that the reduction of the load carrying capacity is due to the additional tensile action introduced by anchoring elements.

In total 18 numerical analyses were conducted for this numerical study. Each of these analyses required about 3 hours of computer time on IBM PS/2 Model 80 computer under DOS operating system. Considering the time and costs required for laboratory experiments of this type the computer simulation appears as being a very efficient tool for such investigations. However, the computer results must always be cautiously verified, which is most reliably done by experiments.

7. CONCLUSIONS

Computer program SBETA, which is based on the nonlinear elastic material model of reinforced concrete, can adequatly simulate the behavior of reinforced concrete beams with anchoring elements. The program is suitable for computer simulation of experiments. Such simulation should be verified and suplemented by experimental investigations.

ACKNOWLEDGEMENT

This research was carried out under the sponsorship of Deutsche Forschungsgemeinschaft, Stuttgart University and Czech Technical University in Prague. The assistance and interst of the sponsors are greatly appreciated.

References

[1] REUTER, M. - Versuch an Plattenstreifen ohne Schubbewehrung bei Einleitung von Lasten über Dübelbefestigungen in die Zugzone, Institut für Werkstoffe im Bauwesen, Universität Stuttgart, Bericht No. 1/9-85/13, 1985.

[2] Einfluss der Lasteinleitung über Kopfbolzen auf das Tragverhalten von Plattenstreifen ohne Schubbewehrung, Forschungs- und Materialprüfungsanstalt Baden-Württemberg, Bericht, Stuttgart, 1985.

[3] REUTER, M., ELIGEHAUSEN, R. - Zulässiger Anteil der durch Befestigungselemnte in die Zugzone einleitbaren Lasten an der Gesamtbelastung von Stahlbetonbauteilen ohne Schubbewehrung, Institut für Werkstoffe im Bauwesen, Universität Stuttgart, Bericht No. 1/17a - 86/18, 1986.

[4] CERVENKA, V., ELIGEHAUSEN, R., PUKL, R. - SBETA Computer Program For Nonlinear Finite Element Analysis of Concrete Structures, Part 1, Program Description, Part 2, User's Manual, Part 3, Examples of Applications, Institut für Werkstoffe im Bauwesen, Universität Stuttgart, 1989.

[5] KUPFER, H., GERSTLE, K.H. - Behavior of Reinforced Concrete under Biaxial Stress, Eng. Mech. Div., ASCE Vol. 99, No. EM4, August 1973, pp. 852-866.

[6] GUPTA, A.K., AKBAR, A. - Cracking in Reinforced Concrete Analysis, J.Struct.Engnrg., ASCE, 99(4),1735-1746.

[7] VECCHIO, F., COLLINS, M.P. - The Response of Reinforced Concrete to In-plane Shear and Normal Stresses, ISBN 0-7727-7029-8, Pub. No. 82-03, University of Toronto, Toronto, Canada, 1982.

[8] BAZANT, Z.P. - Mechanics of Distributed Cracking, Appl.Mech. Rev., ASME, 39 5), 675-705, 1986.

[9] VOS, E. - Influence of Loading Rate and Radial Pressure on Bond in Reinforecd Concrete, Dissertation, Delft University of Technology, 1983.

[10] KOLMAR, W. - Beschreibug der Kraftübertragung über Risse in nichtlinearen Finite-Element-Berechnungen von Stahlbetontragwerken, Dissertation, Techn. Hochschule Darmstadt, 1985.

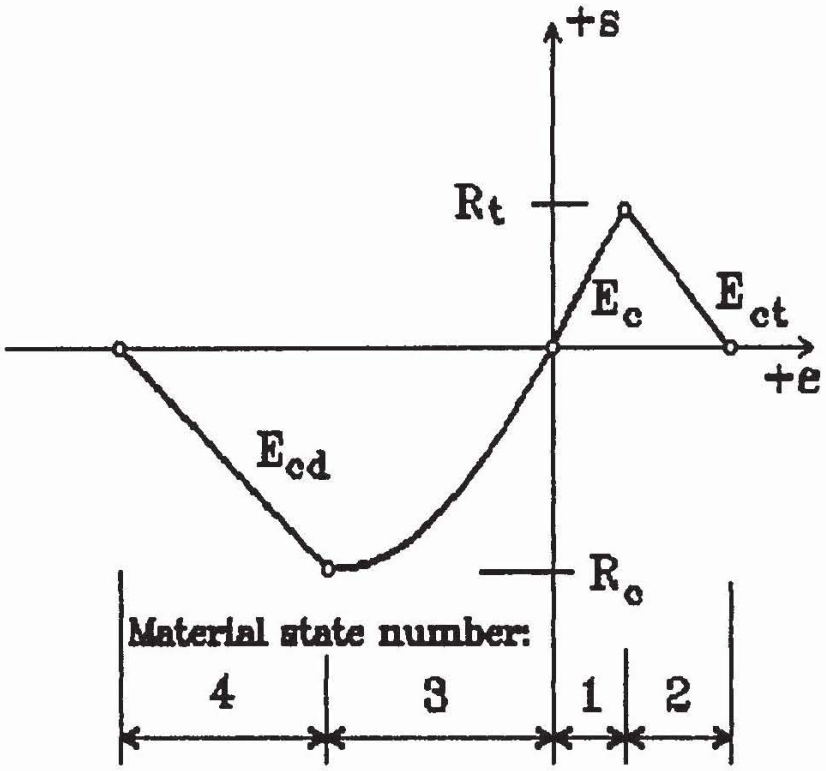

Fig.1 Concrete stress-strain diagram.

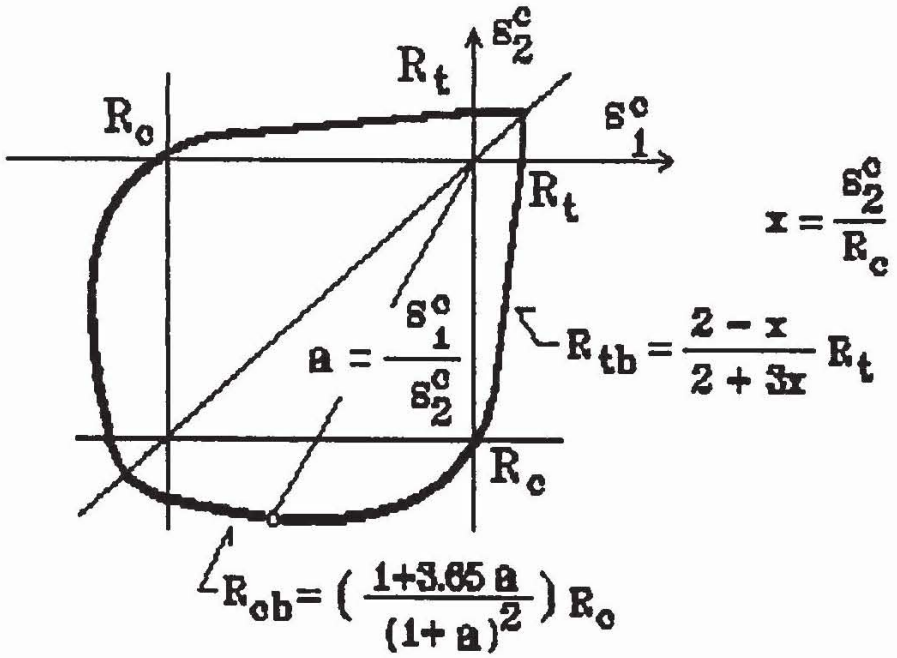

Fig.2 Concrete bi-axial failure function.

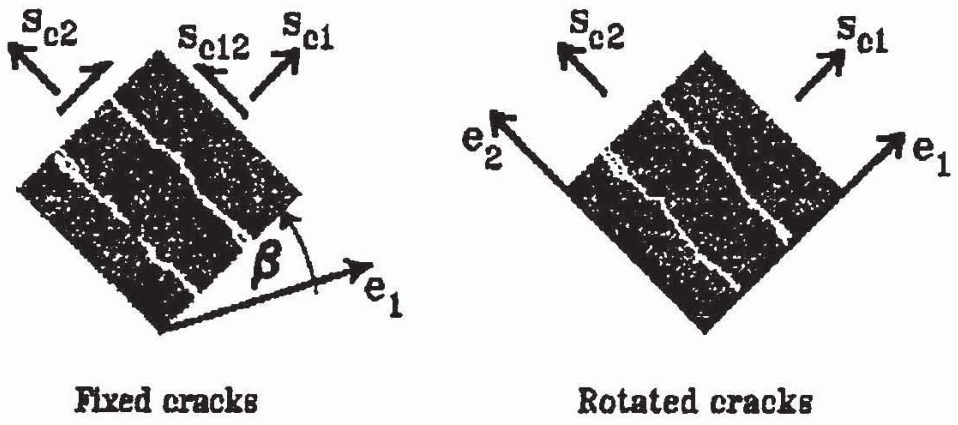

Fig. 3 Crack models with stress components.

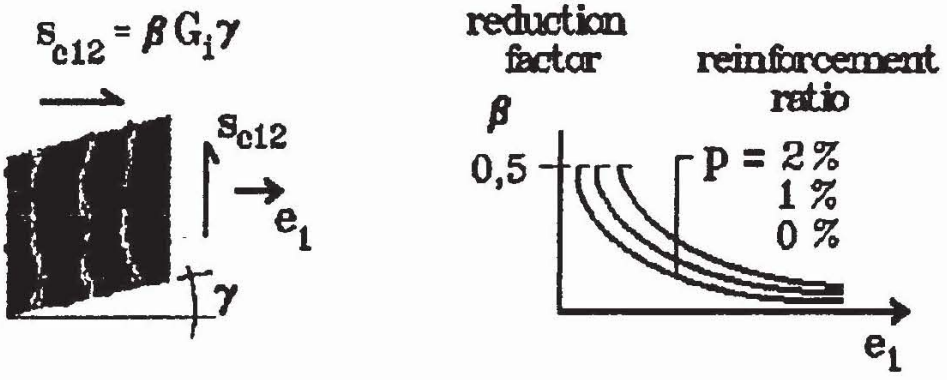

Fig.4 Shear stiffness factor
in cracked concrete.

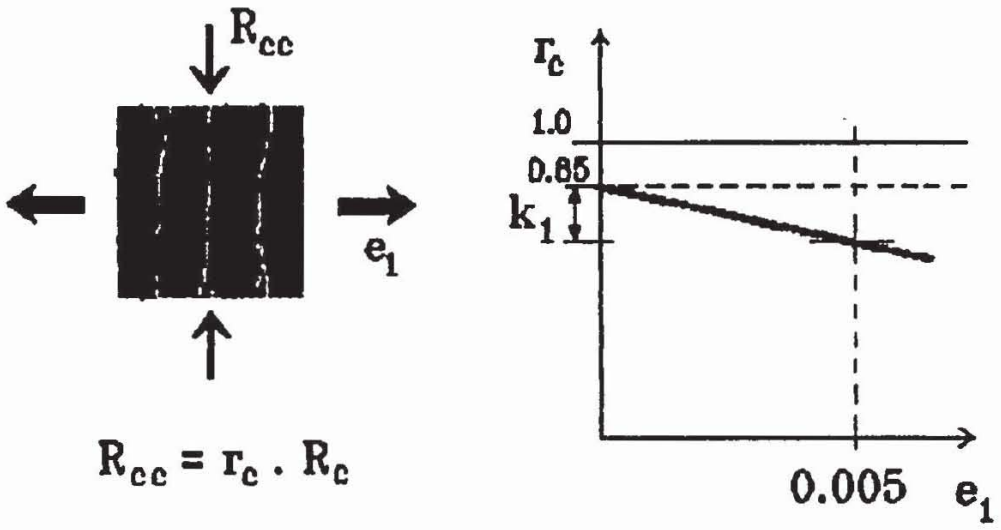

Fig.5 Reduction of compresive strenght R_c.

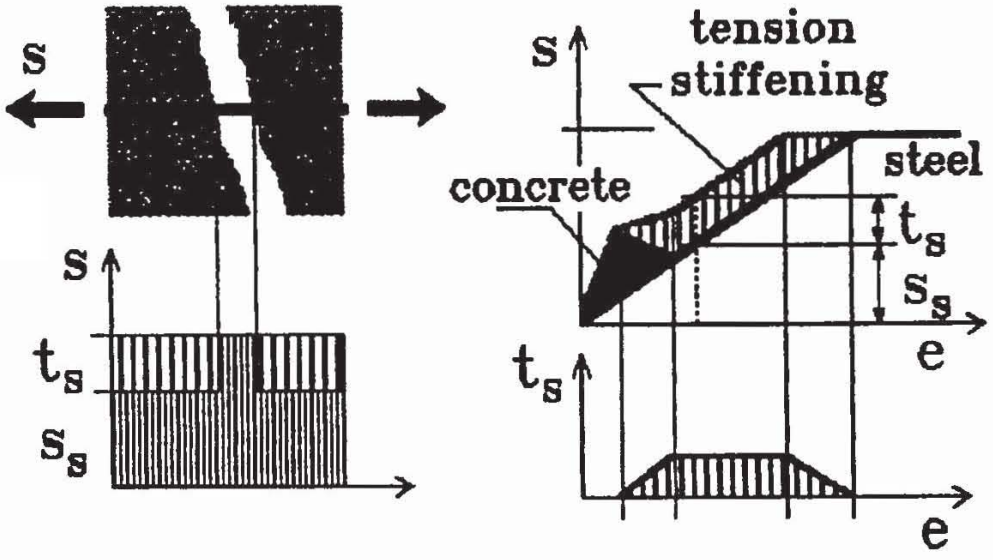

Fig.6 Tension stiffening effect.

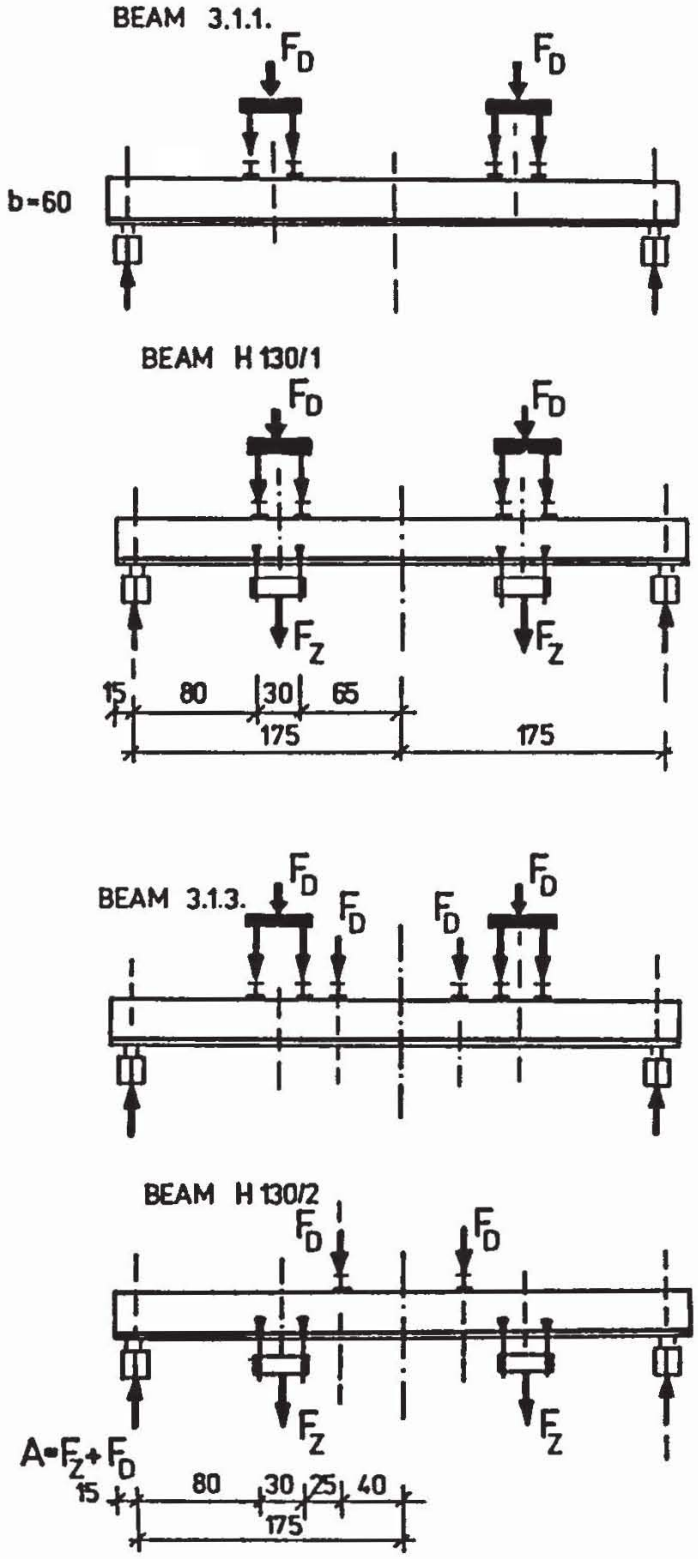

Fig.7 Four experimental beams (dimensions in cm).

P = 0.24 Pmax

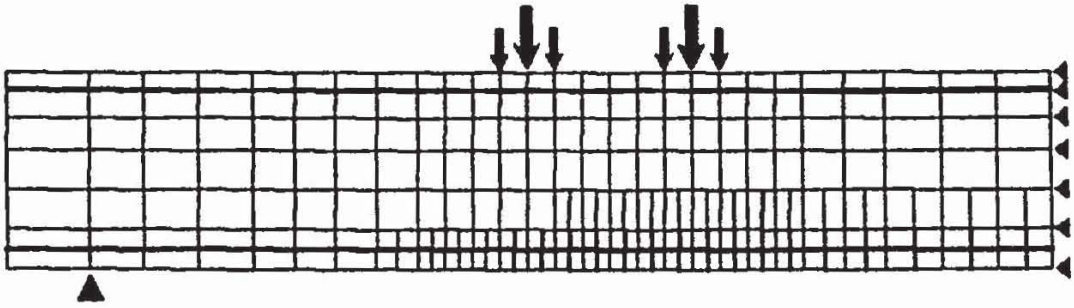

P = 0.64 Pmax

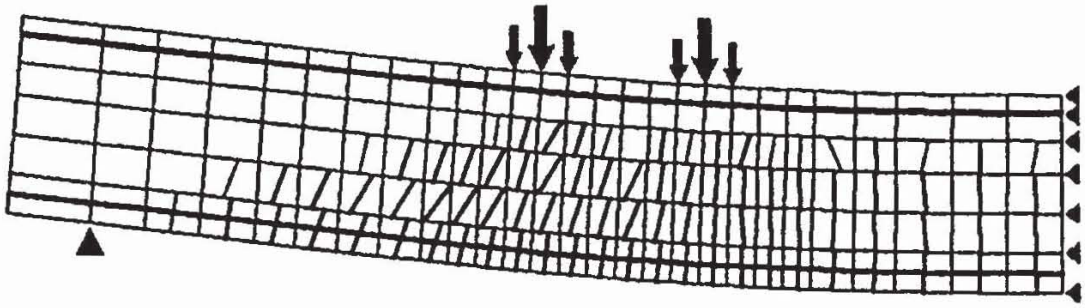

Displacements in deformed mesh multiplied by 10.

P = 0.99 Pmax

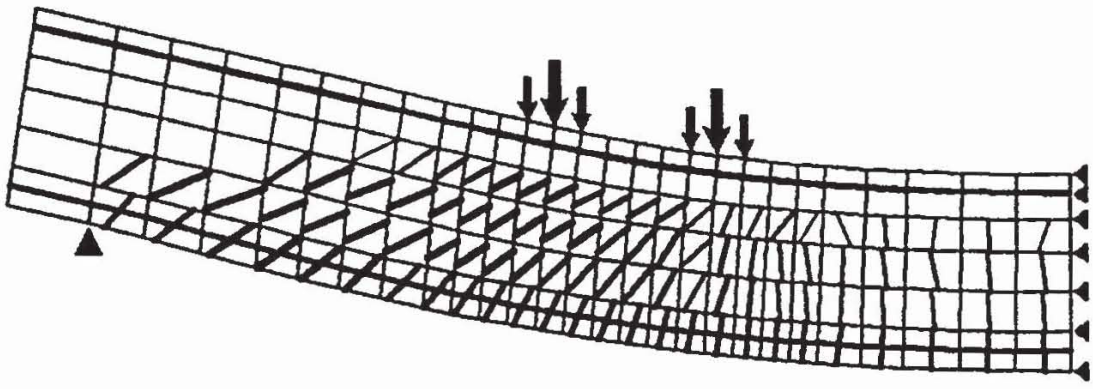

Fig.8 Beam 3.1.1. FEM results in three load stages. Rotated crack model.

fixed cracks

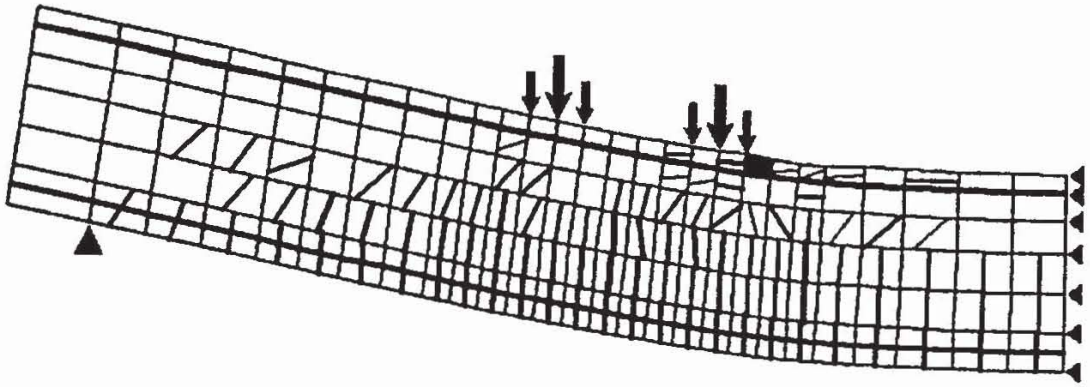

rotated cracks

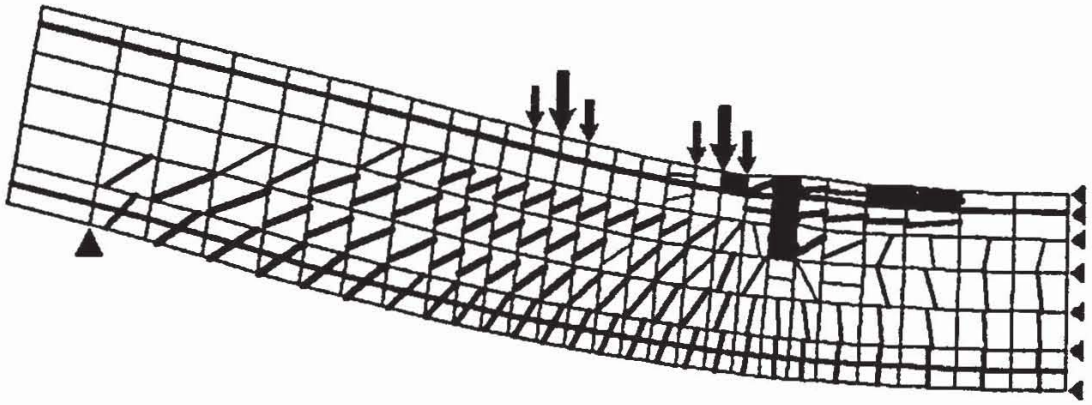

experiment

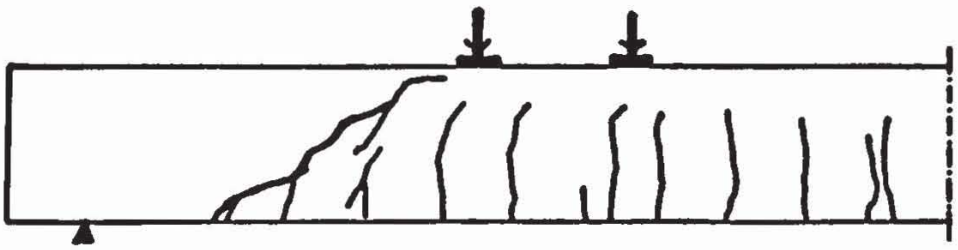

Fig.9 Beam 3.1.1. Comparison of FEM analyses with experiment. FEM model: 162 elements, 196 nodes.

fixed cracks

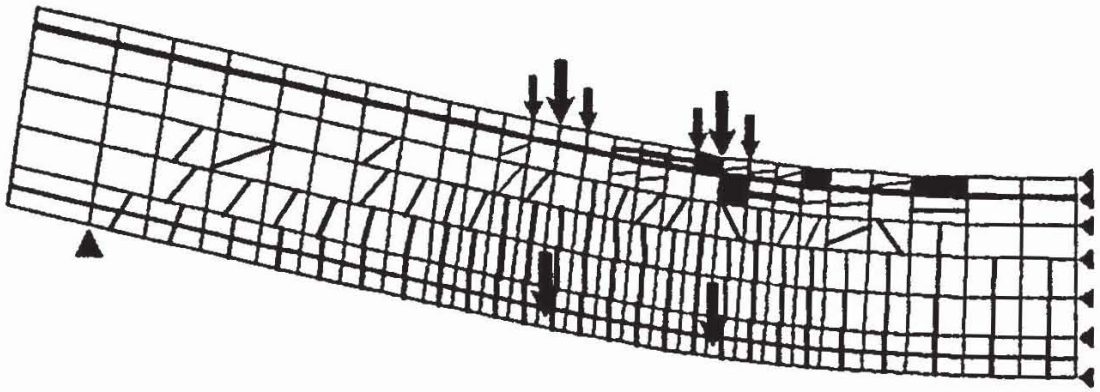

rotated cracks

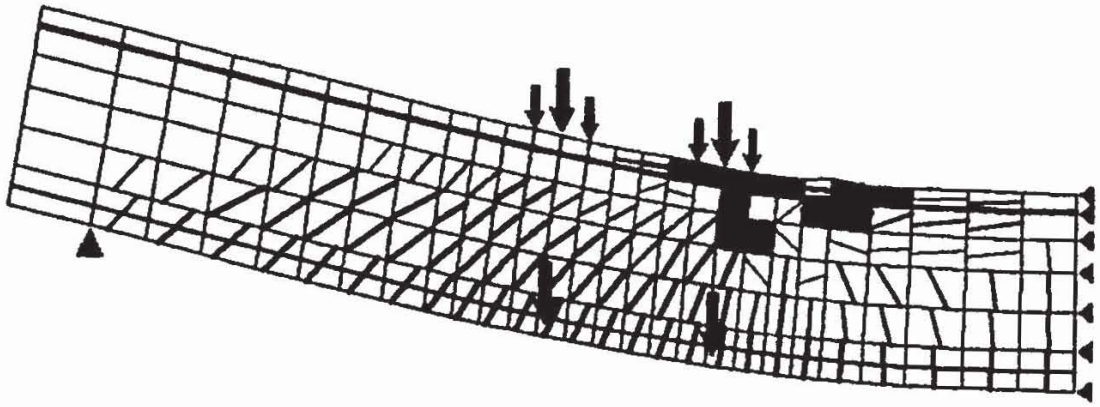

experiment

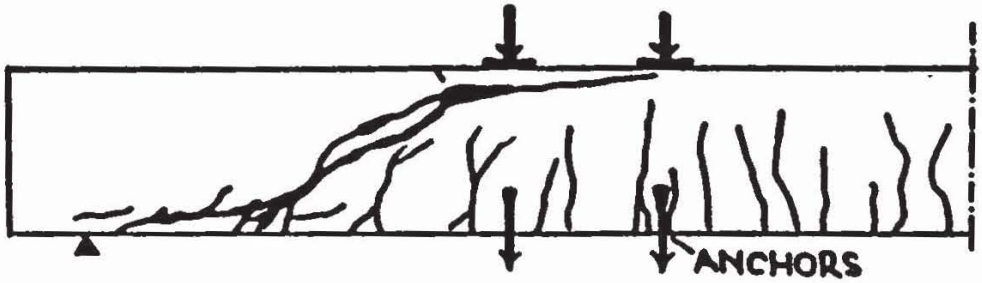

Fig.10 Beam H130/1. Comparison of FEM analyses with experiment. Combined top and anchor loading.

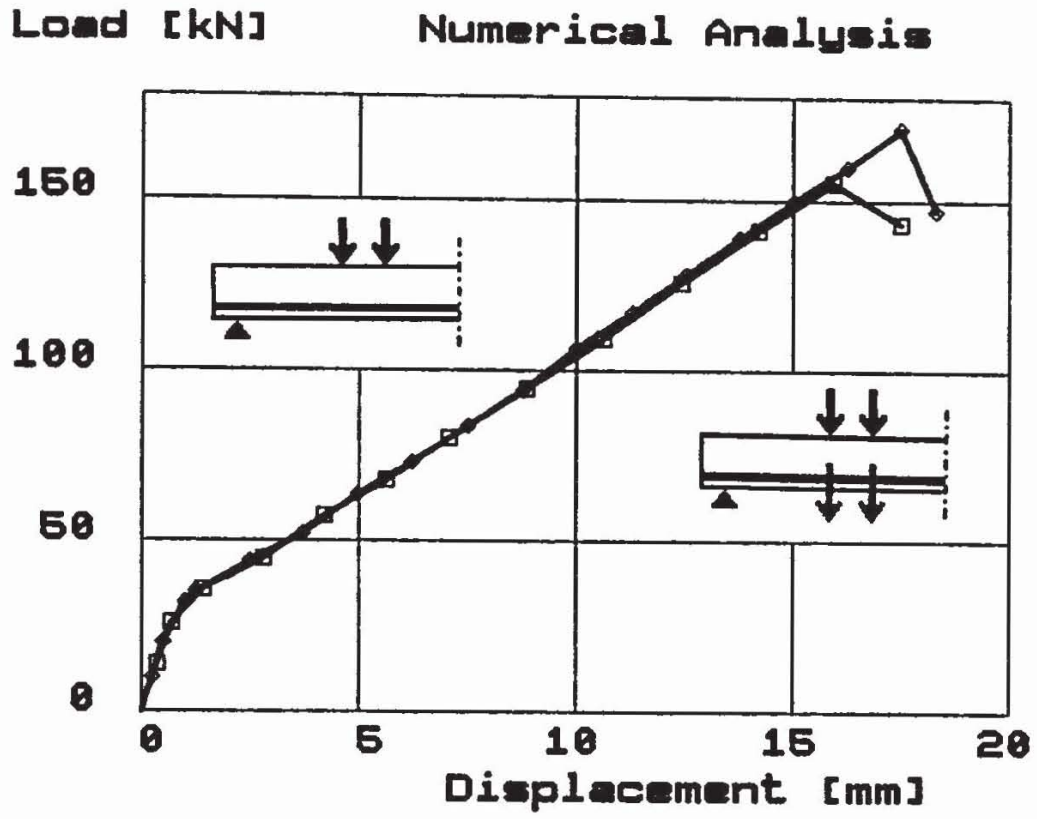

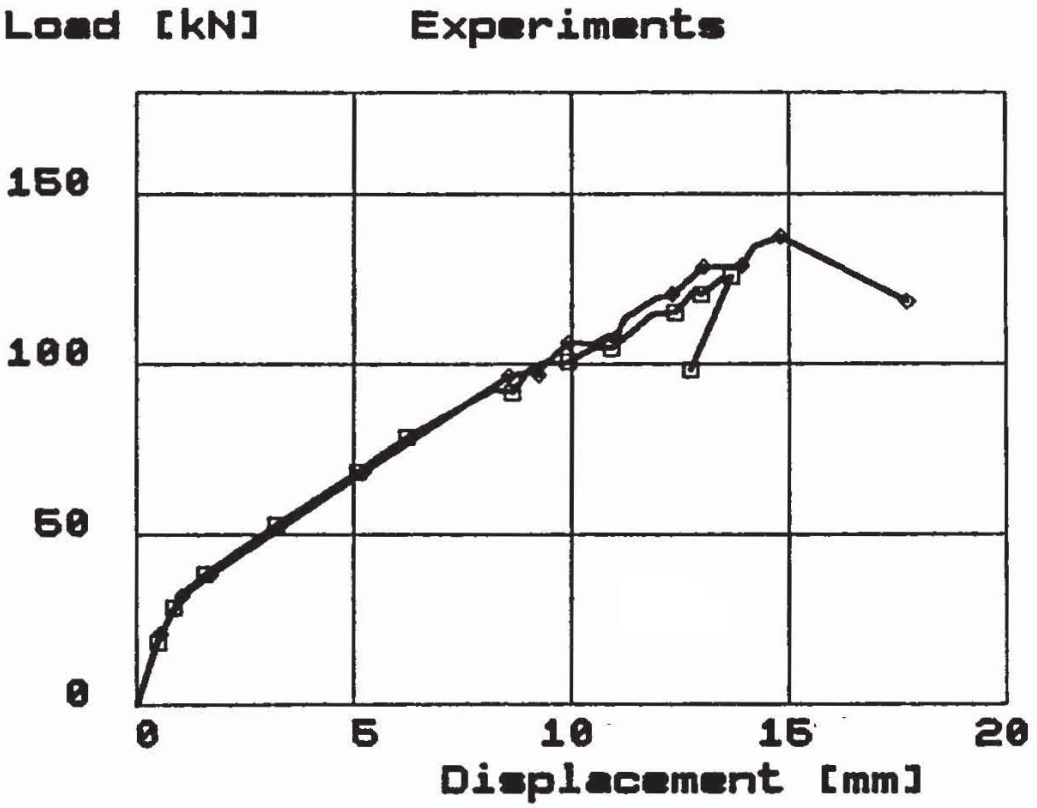

Fig.11 Comparison of FEM and experimental load-displacement diagrams for Beams 3.1.1 and H130/1.

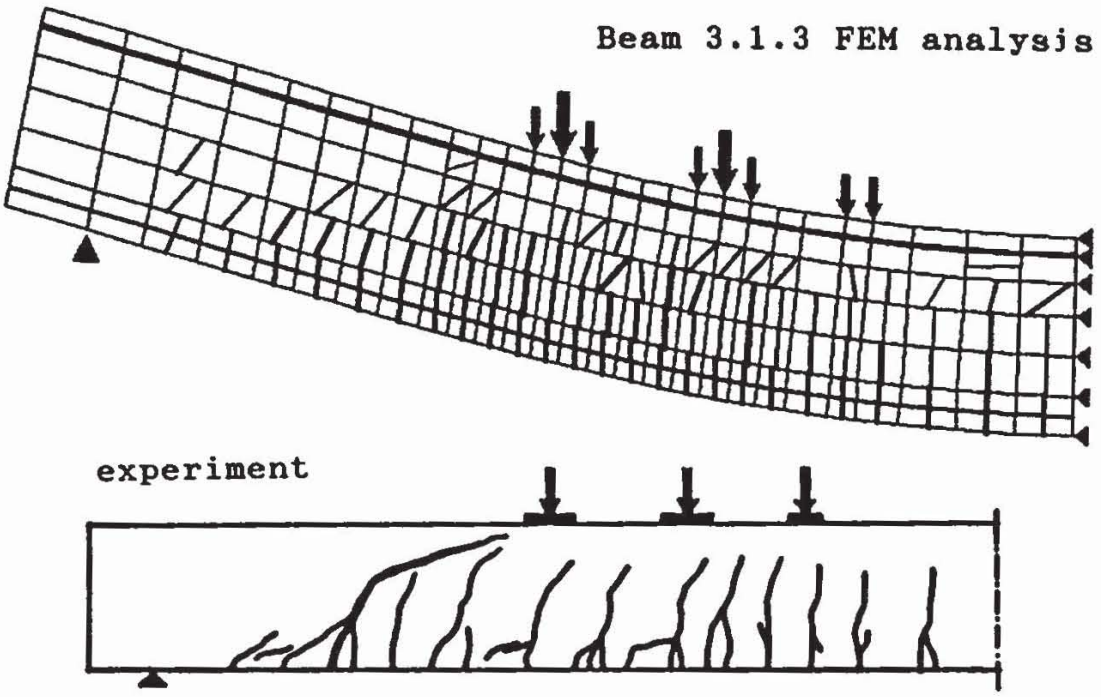

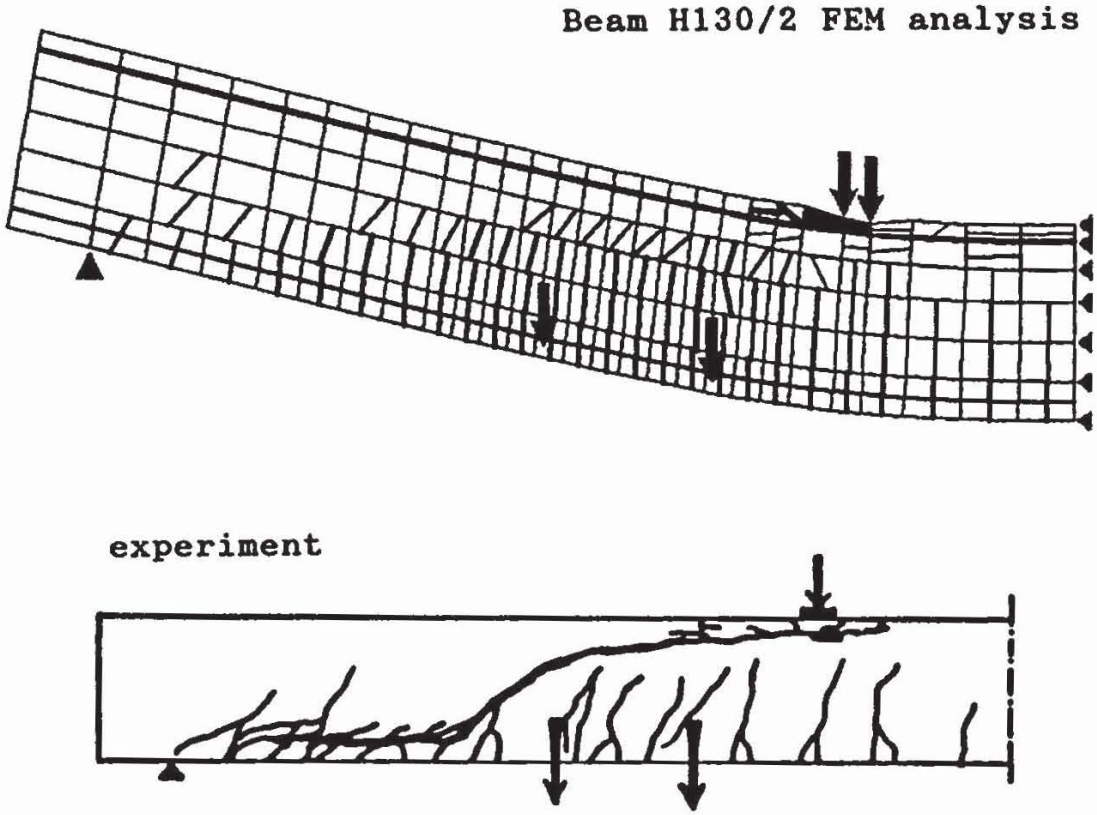

Fig.12 Comparison of FEM and experimental crack and failure patterns for Beams 3.1.3 and H130/2.

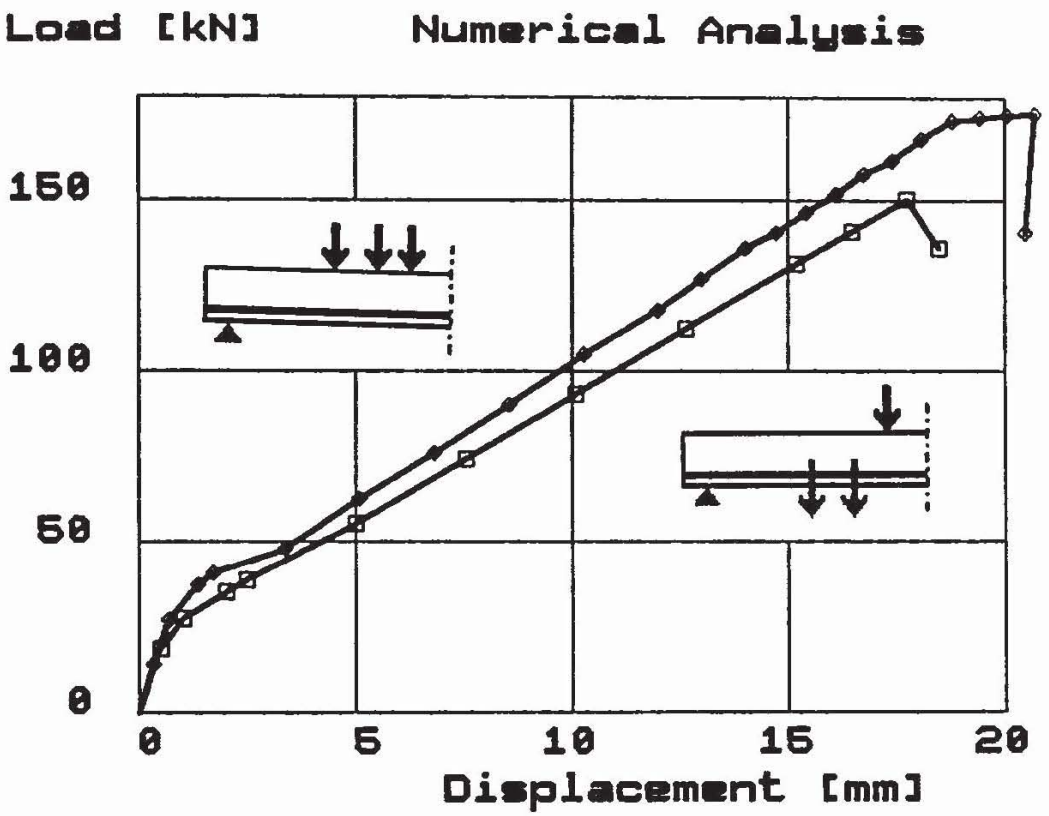

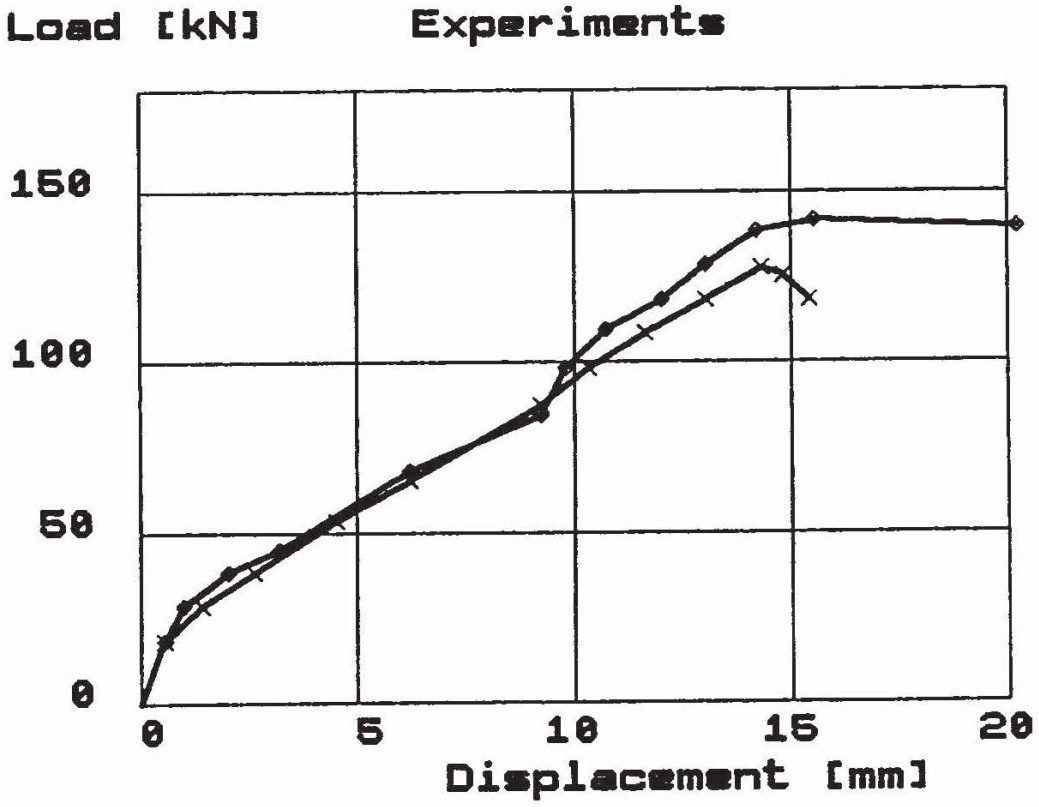

Fig.13 Comparison of FEM and experimental load-displacement diagrams for Beams 3.1.3 and H130/2.

top loading

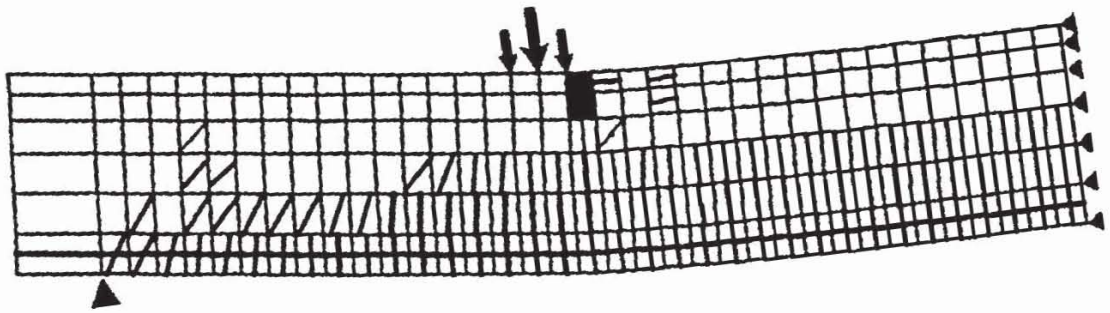

top + anchor loading

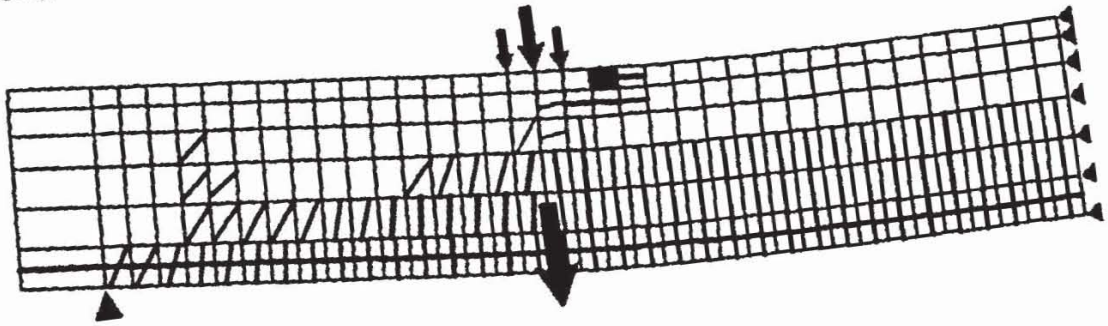

anchor loading

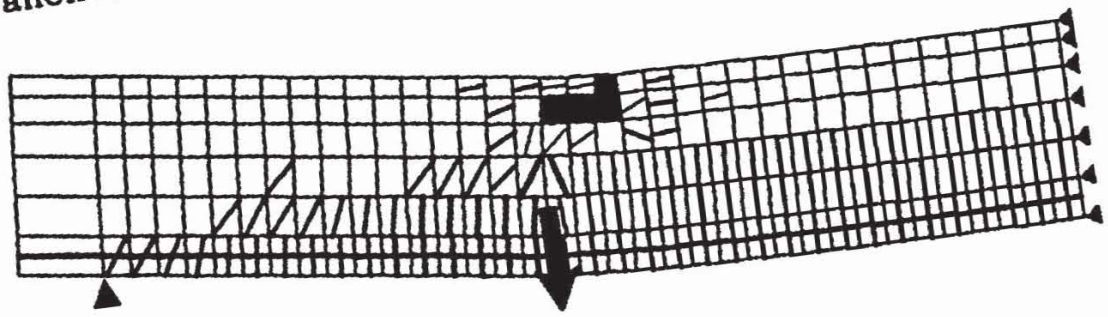

Fig.14 Parameter study. Example of calculated failure states for three types of loading.

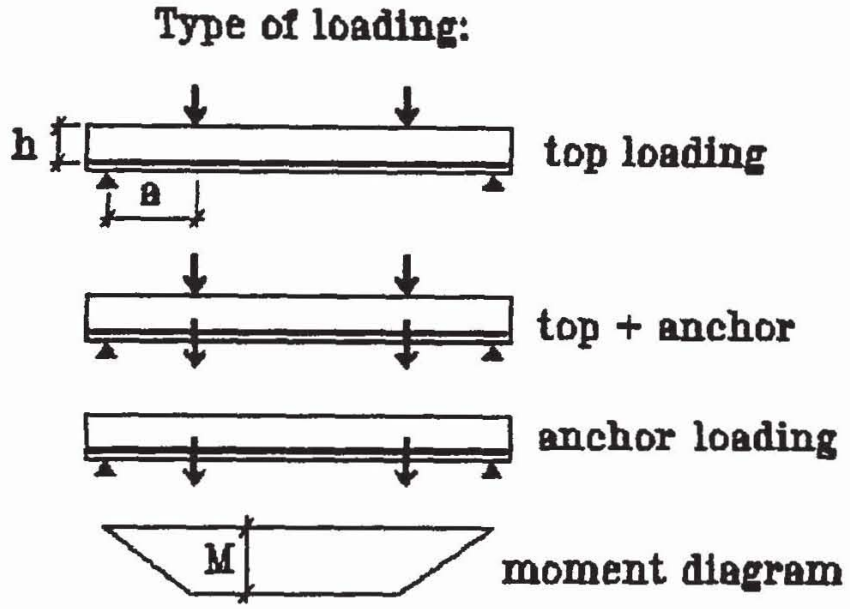

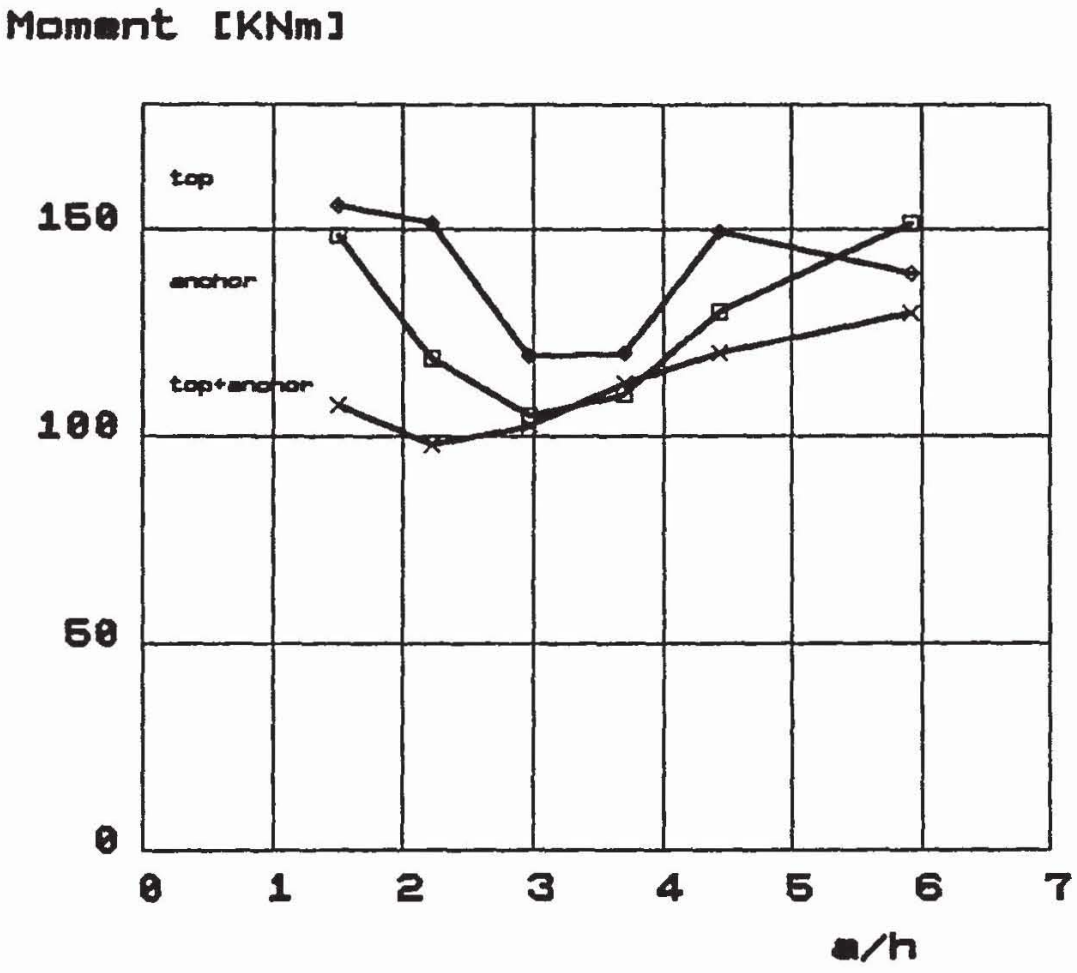

Fig.15 Computer simulation of experiments.
Ultimate moment reduction due to shear failure.